THE FLOW FIELD OF A TWO-BLADED HORIZONTAL AXIS TURBINE VIA COMPARISON OF RANS AND LES SIMULATIONS AGAINST EXPERIMENTAL PIV FLUME MEASUREMENTS

Danny Sale[1], Alberto Aliseda
University of Washington
Dept. of Mechanical Engineering
Seattle, WA, U.S.A.

[1]corresponding author: dsale@uw.edu

ABSTRACT

Experiments and numerical simulations are conducted for an array of axial-flow Marine Hydro-Kinetic (MHK) turbines operating in a flume. This study aims to understand the influence of coherent structures in high Reynolds number wakes on energy extraction and dynamical rotor control processes. In the flume experiments, rotor torque and rotational position measurements are collected, and the flow field is characterized by simultaneous imaging with particle image velocimetry. The performance of 3 turbines are characterized under varying stream-wise spacing and cross-stream offsets. To study the effect of unsteady hydrodynamics, the turbines are outfitted with either open-loop or close-loop feedback rotor-speed controller. In the numerical simulations, turbine models within the class of "actuator methods" are included from Large-Eddy-Simulations and Reynolds-Averaged-Navier-Stokes methods, where these turbine models impose body forces upon the flow field in form of disks or lines.

1. INTRODUCTION

Turbine efficiency and wake structure of a small array of 3 model-scale Marine Hydrokinetic (MHK) turbines, inspired by the DOE Reference Model 1 (shown in Figure 1), were measured in a large recirculating flume. The experimental results were compared against Computational Fluid Dynamics (CFD) simulations using different models to represent the effect of the rotor and for different strategies to simulate the turbulent flow field: both Large Eddy Simulation (LES) and Reynolds-Averaged Navier-Stokes (RANS).

Objectives:

- Study the Reynolds dependence of the near wake and the influence of the nacelle on the wake structure (with and without yaw angles) from Particle Image Velocimetry (PIV) and Computational Fluid Dynamics (CFD);
- Compare methods of controlling turbine efficiency by measuring turbine performance with both open-loop and closed-loop rotor speed controllers; and
- Compare these experimental measurements against the LES and RANS model results.

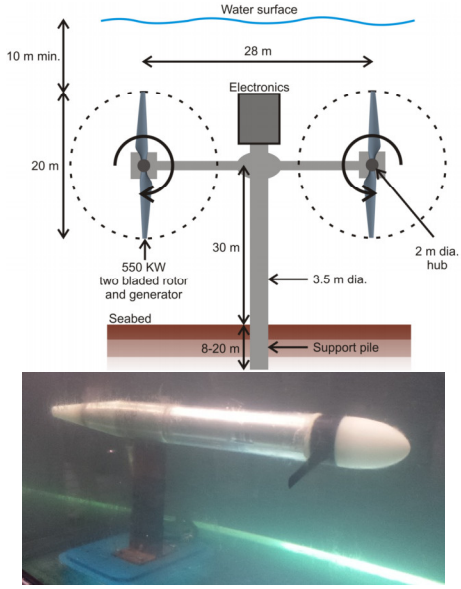

FIGURE 1. TOP: REFERENCE MODELS FOR TIDAL HYDROKINETIC TURBINE [1]. BOTTOM: SCALED DOWN VERSION OF THE TURBINE FOR FLUME TESTING [5].

2. LABORATORY AND NUMERICAL METHODS

2.1 Flume Testing

Experiments were conducted in a large scale recirculating flume located at the Marine Science Center in Bamfield, Canada, (shown in Figure 2). Flow Reynolds number is controlled by maintaining constant temperature in the flume via a chiller, and control of

four pumps. The flume test section is approximately 12.3 meters long, 0.98 meters in width, and 0.76 meters in depth; and current speed can reach up to 1.25 m/s. The flume is instrumented with Acoustic Doppler Velocimeters (ADV) to measure upstream mean flow velocity and turbulence characteristics, and Particle Image Velocimetry (PIV) to resolve the spatial structure of the turbine wakes. The raw ADV and PIV data are relatively clean on modern hardware. Applying common practices in de-spiking the ADV data [6], and filtering the PIV images [7] gave more confidence in the measurement analysis.

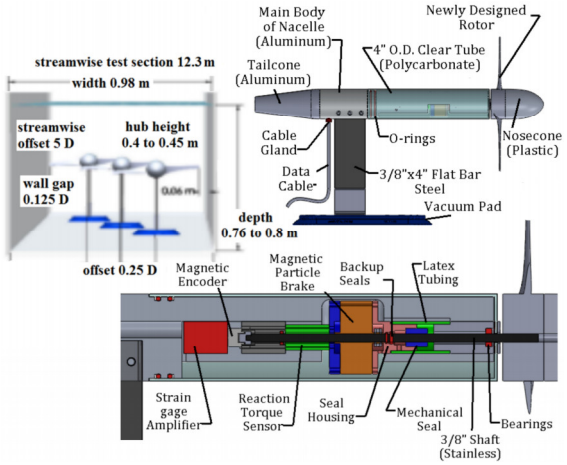

FIGURE 2. THE FLUME IN BAMFIELD MARINE SCIENCE CENTRE, CONFIGURATION OF THE THREE TURBINE ARRAY, AND SOLID MODEL OF RE-DESIGNED TURBINE AS BUILT [5].

2.2 RANS Model (STAR-CCM+)

The Virtual Disk Model (VDM) in Star-CCM+ is an implementation of a few variants on the actuator disk principle. The geometry of the rotating blades is not resolved; instead, the forces on the fluid created by the rotor are modeled as body forces which enter the momentum equations in the form of a source term, distributed over the rotor-swept cylindrical volume. Various distributions of different fidelity are possible to model the action of the rotor depending on the application area. In the RANS models there are currently three methods implemented:

- Body Force Propeller (BFP): The required user inputs are a lookup table of flow speed with coefficients of thrust, torque, and efficiency. The radial distribution of the force component follows the Goldstein optimum (an expression for circulation that gives the velocity distribution of the ideal Betz-Prandtl rotor).
- Blade Element Method (BEM): This method takes the blade geometry into account, requiring the blade pre-twist angles and chord lengths as user inputs. Also required are look-up tables of the lift and drag coefficients, as a function of angle-of-attack. The radial distribution of the forces is most realistic in this model, as it follows the lookup table for the aerodynamic coefficients prescribed by the blade geometry.
- 1D Momentum (1DM): The simplest method, which requires a lookup table of coefficients of thrust and torque, as a function of flow speed. The source term accounts for both the axial and the tangential velocity inductions as derived by the "Ideal Horizontal Axis Wind Turbine (HAWT) theory" with wake rotation.

Several turbulence models have been tested, in order of increasing fidelity: "SST k-Omega", "Two-Layer Realizable k-Epsilon", and "Reynolds Stress Transport". With these turbulence models, the approximation of the boundary layer is handled via the "all *Y+*" wall model in STAR-CCM+, and the meshes are tested to maintain a range of *Y+* within ~30 to 300 to model the turbulent boundary layer (within the buffer layer) along the flume wetted perimeter, and over the geometry of the turbine nosecone and nacelle (included via the overset mesh capability).

Each of the three VDM methods has the same meshing requirements. A main advantage of the VDM is that a coarse mesh around the rotor is sufficient to reproduce near and far-field wakes: only ~20 to 40 cells across the disk is usually sufficient. Mesh cells are very small on the nacelle, so the adjacent rotor zone is also over-refined due to the small mesh size requirements of including the nacelle via overset meshing. The RANS meshes presented here are ~2 million cells total, with ~40 mesh cells along the blade radius length (spacing of ~0.005 meters), as well a value of *Y+* within ~30 was desired on the nacelle surfaces, and the "all Y+" wall model blends the solution from regions of the mesh that become over-resolved (below the buffer layer).

Specification of the inlet turbulent length scale had a large influence on the simulated turbine wakes. Computing the velocity correlation length from the upstream ADV measurements was essential to specifying the correct CFD turbulent length scale at the inlet boundary condition. Using a value of ~0.25*Radius for the characteristic turbulent length scale in the CFD models provided best experimental-agreement with the PIV and torque measurements.

2.3 LES Model (OpenFOAM)

The LES is implemented within the SOWFA OpenFOAM code, developed by the National Renewable Energy Laboratory [2], which models turbine blades, towers, and nacelles as actuator lines (either rotating or stationary body forces). The parameters of the LES actuator-line are: 30 blade elements, with equal radial spacing of 6.5 millimeters, and following references on "best practices" for body force spreading (isotropic Gaussian spreading) [2]. The LES simulation is coupled to an unsteady Blade-Element method, with enabled Beddoes-Leishman dynamic stall model and Glauert hub-tip loss models, to compute the total force distribution along the span of the blade used in the actuator line source term.

A turbulence inflow generator is used to impose the correct inlet boundary conditions for the LES simulation. This requires specification of the Reynolds stresses, measured from the ADV three velocity components at the inlet. The generator then produces

turbulence time series with the correct correlations and conservative flow fields for the LES to evolve inside the domain [3].

In the LES, three different levels of resolution (coarse/medium/fine) were tested in an effort to determine the optimal resolution that guarantee grid independence. Medium resolution level uses [Nx Ny Nz] = [930 100 80], thus 7,440,000 cells with a uniform mesh spacing of 0.010 meters. To safely satisfy a stable blade-tip Courant–Friedrichs–Lewy (CFL) condition, the time step used was 0.00125 seconds (800 Hz). LES-fields were saved at 50 Hz (every 16 time steps in the 2nd-order accurate numerical integration).

3. SAMPLE RESULTS

3.1 Single Turbine

A single MHK turbine was tested at tip-speed-ratios from ~5 to ~12, and at three flume current speeds, to evaluate Reynolds number dependency of the results. The effect of the turbine nacelle was of particular interest in the single turbine study. Resolving the near wake behind an individual MHK turbine to validate the LES and RANS wake simulations was also a contribution of this study. Particle Image Velocimetry measurements of the near wake are shown in Figures 3 to 8, the fields of view are positioned at 0, 2, and 4 rotor diameters downstream relative to the blade rotor plane.

Figure 3 shows PIV of a single turbine wake, identifying the decay of the tip vortex, hub vortex, and shear layer separating the wake from the free stream. Figure 4 is a line integral convolution (LIC) of the Reynolds decomposed fluctuating velocity field; this was also successful to identify coherent structures like the tip vortex.

A comparison of the PIV with the RANS (1DM), and LES (with and without turbulent inlet condition) is shown in Figure 5. Note that the LES cases did not yet include the presence of the nacelle, and that longer runs are needed for the LES simulations to develop an accurate ensemble mean for direct comparison to the PIV and RANS; only a snapshot of the unsteady simulations is shown here (currently had been run up to 15 seconds of simulation time). The wake of the LES persists to much greater distances downstream compared to the PIV and RANS results. Without ambient turbulence, the uniform inlet LES looks similar to the averaged fields. When a turbulent inlet condition is added, wake meandering and faster decay are observed.

Results from the case where the turbine was at a yaw angle of 20 degrees to the flow, are shown in Figures 6 to 8. Figure 6 compares the mean velocity and vorticity fields, identifying similar features to that of Figure 3 and, in addition, highlights the presence of the nacelle, which acts like a cylinder in crossflow. The additional wake from the nacelle counter-rotates to the adjacent tip vortex, and the direction of the bulk wake shifts slightly off the streamwise direction. To further study the effect of Reynolds number, the flume speed was increased from 1.0 to 1.2 m/s; turbulence intensity was

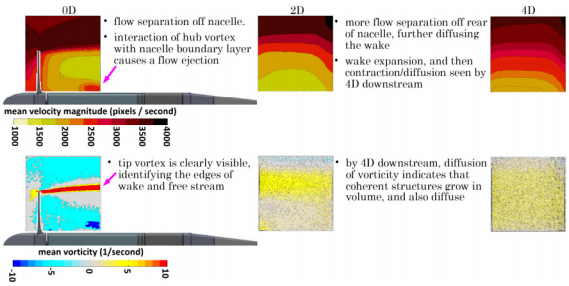

FIGURE 3. MEAN VELOCITY AND MEAN VORTICITY FIELDS IN THE NEAR WAKE OF SINGLE MHK TURBINE.

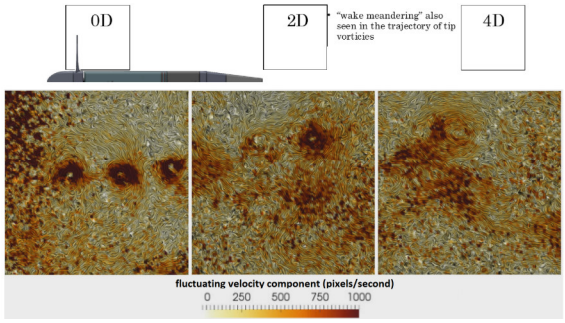

FIGURE 4. SHOWING LINE-INTEGRAL-CONVOLUTION (LIC) OF THE INSTANTANEOUS VELOCITY BASED ON REYNOLDS DECOMPOSITION. THE LIC MEANS TO ADVECT A RANDOMIZED TEXTURE WITH THE VECTOR FIELD. IN THIS CASE THE TIP VORTICES CAN BE SEEN IN THE THREE FIELDS OF VIEW (THE FASTEST AND SWIRLING PARCELS)

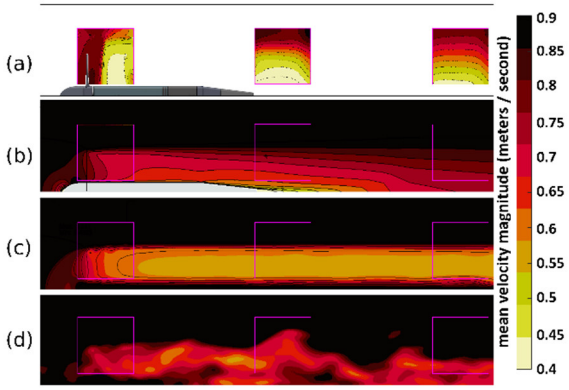

FIGURE 5. COMPARING THE MEAN VELOCITY MAGNITUDE, OBTAINED BY: (A) THE PIV, (B) THE RANS WITH 1DM, (C) LES WITH UNIFORM INLET, AND (D) LES WITH TURBULENT INLET CONDITION. IN VIEWS ABOVE, ONLY HALF THE WIDTH OF FLUME IS SHOWN, AND AT SAME LOCATIONS OF THE PIV FIELD OF VIEW.

~10 percent for both cases. An additional flow structure is observed in Figure 7, by comparison with the flow field in Figure 6, separating possibly off the nacelle or nosecone, as identified by the purple arrow in Figure 7. For the yawed turbine case, a comparison of the PIV with the RANS (1DM), and LES (with and without turbulent inlet condition) is shown in Figure 8. In these cases, the RANS uses the SST k-Omega closure model, and the LES uses standard Smagorinsky sub-grid model.

Figure 9 demonstrates the effect of Reynolds number scaling on the turbine efficiency, as well the performance of the new closed-loop rotor-speed controller which updates the reaction torque of the

particle break (from 1 to 10 Hz) to maintain a target tip-speed-ratio. The large jump in efficiency can possibly be contributed by improved performance of the new controller, and further increase in chord based Reynolds number; and possibly a slight increase of blockage ratio by 1%. At tip-speed-ratio of 7.0, the chord based Reynolds number (at 75% blade span) ranges from 43,000 to 172,000 between the flume speeds tested (0.52 to 0.98 m/s), and for the NACA 4415 hydrofoil this is known to pass through a transitional regime w.r.t. lift and drag sensitivity.

3.2 Array of Three Turbines

CFD simulations were carried out and compared against the 3-turbine array experiments [5]. The performance of the three turbines in a small array is shown in Figure 10. The experimental measurements (open symbols) are compared against simulations using both RANS equations with VDM, Propeller, and BEM rotor models (dashed, dotted, and solid lines), and LES with actuator line model (stars). The most striking feature of these array efficiency measurements is that the middle turbine has lower efficiency than both the front (highest) and the back (second highest) turbines. This is associated with the recovery of the momentum deficit in the wake, induced by the mixing caused by the front and middle wakes in a highly confined (high blockage effect) environment. Thus, the back turbine sees a higher, not increasingly lower, momentum flux through its rotor, than the previous (middle) turbine and can therefore operate with intermediate efficiency (not quite rising up to the level of the front turbine that receives the highest momentum flux). This behavior is captured by both the RANS and LES simulations. The RANS simulations, however, vary widely in their quantitative agreement with the measured efficiency, as well as in the predictions of the trend of efficiency with TSR for this high blockage configuration. The LES produced the best quantitative prediction of the efficiency for all three turbines, although the trend with TSR has not been explored yet. The BEM, 1DM, and LES at least predict the trend that the downstream turbine operates more efficiently than the middle turbine; but there are still large differences when compared to the experimental data, especially as tip-speed-ratios increase beyond ~8 when rotors can enter the "turbulent wake state" or "vortex ring state", at which the rotor produces a wake more similar to a bluff body flow. In these states vibration and buffeting can occur, leading to increased frequency of vortex shedding. For a wind/hydrokinetic turbine this interval is reached at high tip speed ratios (i.e. low flow speeds) and it is unlikely that the turbine will operate well in this regime as this state is quite unstable (except as a short transient). The increased turbulence in the wake is efficient at mixing low velocity fluid in the wake with the faster moving fluid in the surround ambient flow. By this mechanism, momentum is transferred into the wake; and the wake expands while the velocity deficit is reduced. Blockage effects further contribute to this kind of turbulent mixing. At high flow speeds, hence lower tip-speed-ratios, the blades enter hydrodynamic stall regime and also become unstable and inefficient as a result.

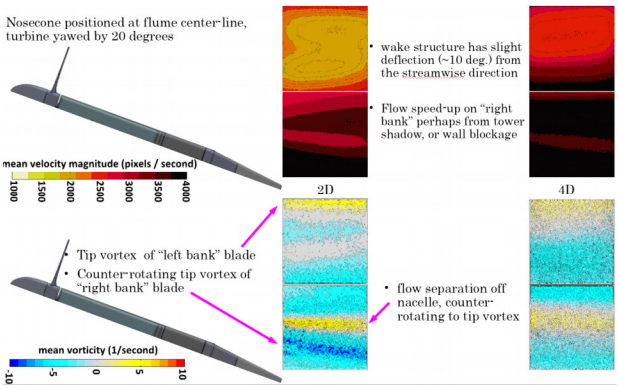

FIGURE 6. SHOWING INSTANTANEOUS VELOCITY AND VORTICITY. TIP-SPEED-RATIO OF 7.0, FLUME SPEEDS AT 0.9 M/S, YAW ANGLE 20 DEG. WHEN THE MHK TURBINE IS ANGLED FROM THE INCOMING FLOW THE WAKE IS STEERED AND FURTHER DESTABILIZED BY THE FLOW SEPARATION COMING FROM THE NACELLE.

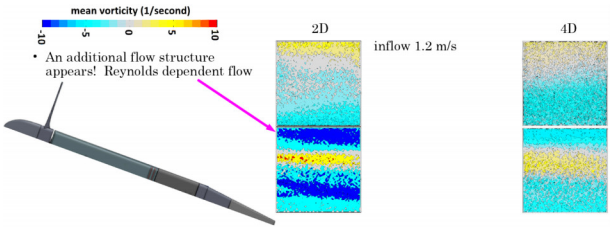

FIGURE 7. INCREASING THE REYNOLDS NUMBER CREATED AN ADDITIONAL FLOW STRUCTURE SEPARATING OFF THE NACELLE OR NOSECONE.

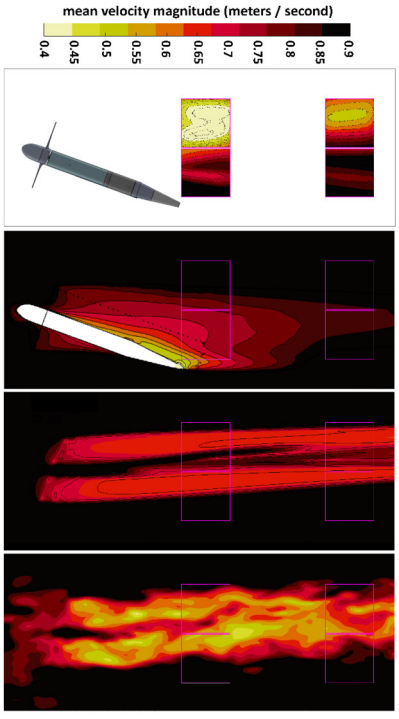

FIGURE 8. SHOWING PIV, RANS, AND LES FOR THE YAWED TURBINE CASE. THE FULL WIDTH OF FLUME IS SHOWN, AND AT SAME LOCATIONS OF THE PIV FIELD OF VIEW.

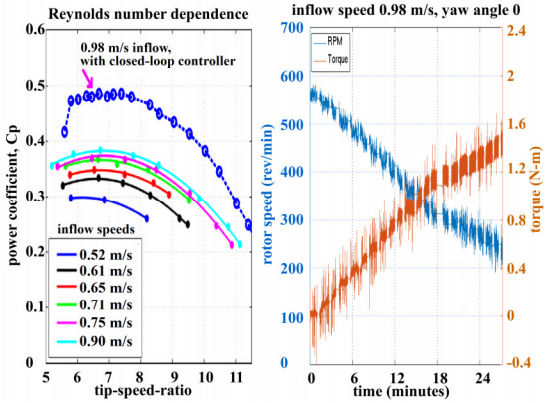

FIGURE 9. EXPERIMENTAL MEASUREMENTS OF TURBINE EFFICIENCY (LEFT) AND TORQUE (RIGHT) AS A FUNCTION OF TIP SPEED RATIO AND ANGULAR SPEED, RESPECTIVELY.

Notice that the RM1 design had a nominal peak in efficiency at a TSR of 7.0, but both experiments and simulations showed peak efficiency at higher TSR (7.5 to 8). This is consistent, however, with the high blockage ratio (up to 21%.) at which these experiments and simulations were conducted. At high blockage, the induction velocity imposed by the presence of the turbine on the free stream as it approaches the rotor plane is less marked, making the turbine operate with a higher effective velocity at the rotor plane than in a confinement-free conditions. Thus, the effective angle of attack (which is the arctangent of the speed at the rotor divided by the rotational speed, $V/(\Omega R)$, for optimum lift (and efficiency) is reached at a higher angular velocity, and therefore higher tip speed ratio than nominal.

4. CONCLUSIONS

A laboratory scale MHK turbine (designed, manufactured and flume tested) demonstrated high efficiency and wake characteristics similar to the full scale reference model turbine (Figure 1). The dataset covers tip-speed-ratios from cut-in speed to peak efficiency, to onset of stall; covering the range of to windmill (peak efficiencies) turbulent wake state and vortex-ring state (where rotors act more like wakes of bluff bodies and increase mixing). Differences between the PIV, RANS, and LES confirm that the turbine models have certain strengths and shortcomings. Namely, the overset mesh method performs well to capture the wake of nacelle, while the LES does not include the nacelle effect and therefore predicts the wake inaccurately. Adding a turbulence inflow to the LES greatly improves the realism of the model, showing near wake breakdown and wake meandering, which was observed here and has been observed in other MHK and wind turbine studies [4]. A marked improvement in efficiency was seen, although contributed by several factors such as: the new rotor-speed controller, Reynolds scaling, and blockage effects. Source codes developed in this report are available at [8].

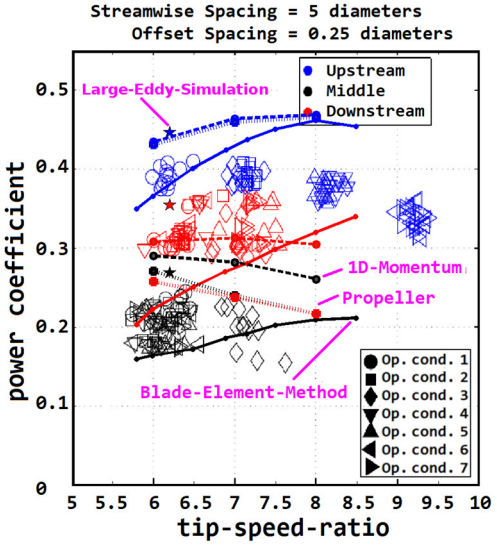

FIGURE 10. (TOP): COMPARISON OF THE RANS VIRTUAL DISK METHODS TO THE LES ACTUATOR LINE METHOD FOR THE THREE-TURBINE LATERAL OFFSET CASES, AGAISNT THE EXPERIMENTS CONDUCTED IN [5]. TIP-SPEED-RATIO IS DEFINED BASED ON THE MOST UPSTREAM INFLOW VELOCITY.

ACKNOWLEDGEMENTS

Thanks to Ben Strom, Rob Cavagnaro, Dom Forbush, John Bates, Michelle Hickner and Brian Polagye for their help setting up and conducting the experiments. This work was financially supported by the National Science Foundation under the Sustainable Tidal Energy project, and the Naval Facilities Engineering Command through the Northwest National Marine Renewable Energy Center. Help from the Bamfield Marine Sciences Centre and specially Eric Clelland is greatly appreciated. This work was facilitated through the use of infrastructure provided by the Hyak supercomputer system at the University of Washington.

REFERENCES

[1] V. Neary, C. Hill, L. Chamorro, B. Gunawan, F. Sotiropoulos, "Experimental Test Plan – DOE Tidal and River Reference Turbines" Technical Report, Oak Ridge National Laboratory, 2012.

[2] M.J. Churchfield, Y. Li, P.J. Moriarty. "A large-eddy simulation study of wake propagation and power production in an array of tidal-current turbines". Phil. Trans. R. Soc. A 28 February 2013 vol. 371 no. 1985

[3] Kornev, N. & Hassel, E. (2007). "Method of random spots for generation of synthetic inhomogeneous turbulent fields with prescribed autocorrelation functions". Communications in Numerical Methods Engineering, Vol. 23, Issue 1, pp. 35-43.

[4] T Javaherchi, S Antheaume, A Aliseda, "Hierarchical methodology for the numerical simulation of the flow field around and in the wake of horizontal axis wind turbines: Rotating reference frame, blade element method and actuator disk model", Wind Engineering, 2014

[5] T. Javaherchi, J. Seydel, N. Stelzenmuller, and A. Aliseda "Experimental and Numerical Analysis of a Scale-Model Horizontal Axis Hydrokinetic Turbine" Marine Energy Technology Symposium, 2014.

[6] V. Neary et al (2011) "Field Measurements at River and Tidal Current Sites for Hydrokinetic Energy Development: Best Practices Manual" Oak Ridge National Laboratory, ORNL/TM-2011/419

[7] R.J. Adrian and J. Westerweel. Particle Image Velocimetry. Cambridge: Cambridge University Press, 2011.

[8] Computer-Aided-Engineering tools for wind, wave, & tidal energy research & development. Northwest National Marine Renewable Energy Center. https://github.com/nnmrec